Journal of Basic and Environmental Sciences, 5 (2018) 252-255

ISSN

Online: 2356-6388

Print: 2536-9202

Research paper Open Access

Preparation and characterization of α-Fe_2O_3 via auto-combustion synthesis

Ayman A. Ali, Mostafa Y. Nassar, Abd elazeem M. El sharkwy, Alaa S. Amin and Esraa A. Abdel Lateif

Chemistry Department, Faculty of science, Benha University, Benha, Egypt

Abstract

Hematite nanoparticles (α-Fe_2O_3) have been successfully fabricated by using auto-combustion method followed by calcination at 600 ºC for one hour. The synthesized iron oxide nanoparticles were characterized by different tools such as X-ray powder diffraction (XRD), Field-emission scanning electron microscope (FE-SEM) and Fourier transform infrared analysis (FT-IR). The average crystallite size of the as-fabricated iron oxide was calculated to be 54 nm. The characteristic absorption peaks at 535 and 450 cm^{-1} correspond to iron-oxygen stretching and bending vibration mode of α-Fe_2O_3, respectively. The FE-SEM photograph displayed that the synthesized hematite nanoparticles are agglomerated in quasi-spherical shapes with hard agglomeration and the average particle size in the range 1 µm.

Received; 3 May 2018, Revised form; 4 Jun 2018, Accepted; 10 Jun 2018, Available online 1 July 2018

Introduction

Simple and mixed metal oxides nanoparticles are used in various applications such as removal of inorganic and organic pollutants from water, information storage, pigment, catalysts, photo electrochemical water splitting, gas sensors, optical, and biomedical devices, magnetic resonance imaging, and drug and gene delivery[1-4]. Different methods have been used in the preparation of simple and mixed oxide nanoparticles such as combustion synthesis [5-13], sol–gel [14-16], hydrothermal [17-19], and precipitation [20-22].

FeO, Fe_3O_4 and Fe_2O_3 are three types of iron oxide nanoparticles. They are considered to be very important materials due to their nontoxicity, low-cost, catalytic activity, biocompatibility and environmentally friendly nature. Ferric oxide (Fe_2O_3) has four crystallographic phases: hematite (α-Fe_2O_3), β-Fe_2O_3, maghemite (γ-Fe_2O_3), and ε-Fe_2O_3. One of these oxides is hematite with a formula α-Fe_2O_3 and a band gap of 2.1 eV [18, 23]. The most stable iron oxide is hematite (α-Fe_2O_3) under normal conditions, and it has been used in the range of applications as catalysis, inorganic pigments, sensors, biomedical materials, adsorbents, photo-catalyst , solar cells, lithium batteries and magnetic recording devices [9, 15, 24, 25]. In the present study, we aimed to prepare hematite nanoparticles by using combustion synthesis. The structure and morphology of the synthesized materials are well characterized by various tools including XRD, FT-IR and SEM.

2. Experimental

2.1. Materials and reagents

All chemicals used in this work were purchased and used as received without any further purification: Ferric nitrate ($Fe(NO_3)_3.9H_2O$; Merck), (company) and cetyltrimethylammonium bromide (CTAB) (($CH_3(CH_2)_{15}N(Br)(CH_3)_3$); Sigma-Aldrich).

2.2. Preparation of iron oxide nanoparticles via combustion method

Ferric nitrate (4.04 g, 0.01 mole) and CTAB surfactant as fuel (1 g, 0.00275 mole) were dissolved in 30 mL distilled water in which the fuel to oxidant molar ratios (1:3.65). The obtained solution was heated with stirring at 80 °C for 10 min to complete the solubility. After homogenization, the solution was heated at 120º C till to transform into a gel. The viscous gel was ignited on hotplate at 250 ºC until auto-ignition was finished in a few minutes with the release of gases and a black reddish ash was obtained. The as-synthesized ash was transferred into furnace and calcinated at 600 ºC for two h to remove the residual organic material and get pure iron oxide nanoparticles.

2.3. Characterization:

Powder X-ray diffraction (XRD) of the products was measured using diffractometer (Bruker; model D8 advance) with monochromnated Cu-Ka radiation, 1.54178 (˚A) in the 2θ range of 10-80º. FT-IR spectra were taken using FT-IR spectrometer (Bomem; model MB 157S) from 4000 to 400 cm^{-1} at room temperature. The morphology and particle size of synthesized sample was obtained using a high transmission electron microscope (HR-TEM, JEOL; model 1200 EX) at an electron voltage of 200 KV and Field emission scanning electron microscope (FE-SEM, JEOL: model JSM-6500F).

3. Result and Discussion

3.1. Powder X-ray diffraction (PXRD)

Fig. 1(a and b) shows XRD patterns of the as-prepared (FC) and calcinated products (FC600). The pattern shows the formation of mixed iron oxide in the form of magnetite

(Fe_3O_4, standard ICSD card no. 89-0691) and hematite (Fe_2O_3, standard ICSD card no. 89-0598) with low crystallinity lines (see Fig.1a). The ratio between magnetite and hematite is equal to 51% and 49%, respectively. Fig. 1(b) displays XRD pattern for iron oxide (Fe_2O_3) after calcination at 600 ºC for one h with high purity without any other phases according to the standard ICSD card no. 89-0598 for hematite[9, 26-29]. The average crystal sizes of iron oxide calculated by using the Debye-Scherrer formula no 1. The estimated average crystal sizes are equal to 29 and 54 nm for the as-prepared and calcinated samples, respectively.

$$D = 0.9\lambda/\beta\cos\theta \qquad (1)$$

where, λ is wavelength (1.5406 A for Cu Kα), θ is the diffraction angle and β is the x-ray full width at half-maximum height of the diffraction peak.

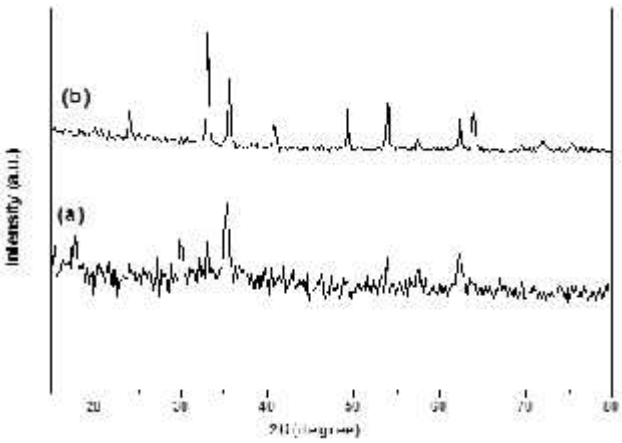

Fig (1): XRD patterns of iron oxide product a) as-prepared and (b after calcination at 600 ºC.

3.2. Fourier transforms infrared analysis (FT-IR)

According to Figure 2, the infrared spectrum (FT-IR) of the prepared iron oxide was in the range of 400-4000 cm^{-1} wavenumber which shows the chemical bonds, as well as functional groups in the compound. The absorption band at 3500−3800 cm^{-1} is corresponding to the stretching vibration of hydroxyl groups, originating from organic material and adsorbed water on the surface of the nanoparticles [5, 30]. The absorption bands at 1390, 1560 cm^{-1} can be assigned to the nitrate, carbon-carbon and carbon-oxygen groups [31]. The characteristic absorption bands for the as-prepared samples (before calcination) appeared at 540, 550 cm^{-1} and shoulder at 640 and 700 cm^{-1} are assigned to Fe-O stretching and bending vibration mode of α-Fe_2O_3 and Fe_3O_4 respectively (see fig.2a) [32]. After calcination as shown in figure2 (b), the characteristic absorption peaks at 535 and 450 cm^{-1}, are corresponding to Fe-O stretching and bending vibration mode of α-Fe_2O_3 respectively[31, 33].

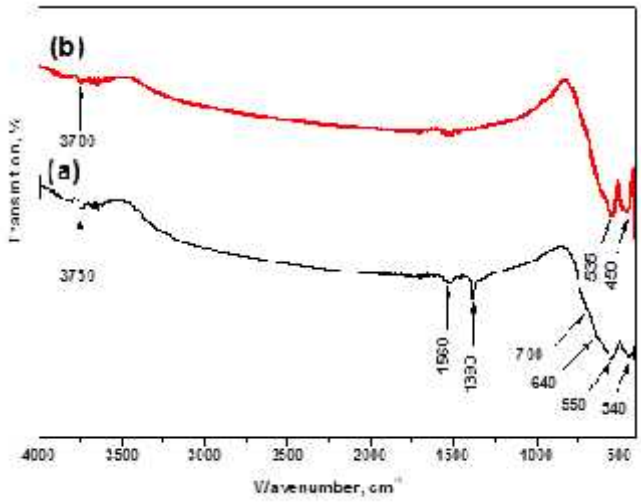

Fig (2): FTIR spectra of iron oxide product a) as-prepared and (b after calcination at 600º C.

3.3. Field-Emission Scanning Electron Microscope (FE-SEM)

The morphology of synthesized iron oxide in the form of hematite nanoparticles was studied by field-emission scanning electron microscope (FE-SEM) as shown in Fig. 3. The FE-SEM micrograph shows that Fe_2O_3 nanoparticles are in form of quasi-spherical and flake-like particles with hard agglomeration and the average particle size in the range 1 µm.

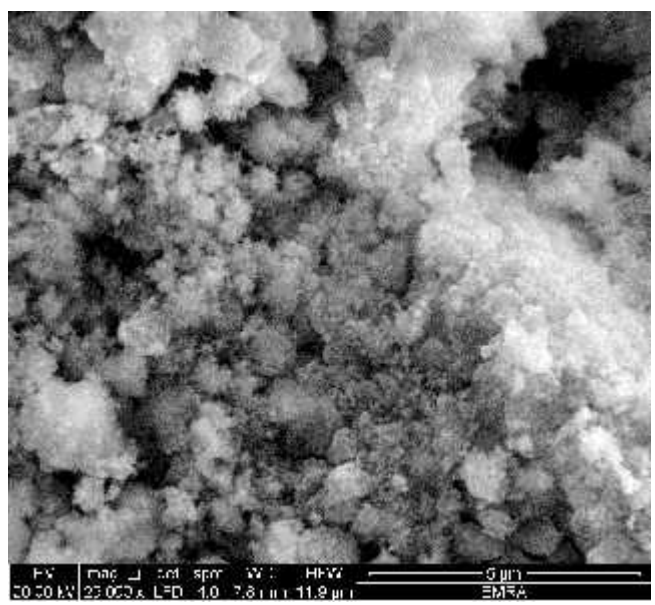

Fig (3): FE-SEM micrograph of iron oxide synthesized after calcination at 600º C.

4. Conclusions

Fe_2O_3 nanoparticles were synthesized by auto-combustion method using ferric nitrate (as an oxidizer) and cetyltrimethylammonium bromide (as a fuel) with the fuel to oxidant molar ratio equals to 1:3.65. The obtained powder samples were characterized by using various tools such as X-ray powder diffraction (XRD), Fourier transform infrared analysis (FT-IR) and field-emission scanning electron microscope (FE.SEM). The XRD pattern of iron oxide sample shows the characteristic peaks of hematite (α-Fe_2O_3) after calcination at 600 ^oC with an average crystallite size of 54 nm. The characteristic absorption peaks at 535 and 450 cm^{-1} are attributed to Fe-O stretching and bending vibration mode of α-Fe_2O_3, respectively. The FE-SEM photograph displayed that the synthesized hematite nanoparticles show the quasi-spherical shapes with hard agglomeration and the average particle size in the range 1 µm.

References

[1] M.Y. Nassar, T.Y. Mohamed, I.S. Ahmed, I. Samir, MgO nanostructure via a sol-gel combustion synthesis method using different fuels: an efficient nano-adsorbent for the removal of some anionic textile dyes, J. Mol. Liq., 225 (2017) 730-740.

[2] M.Y. Nassar, T.Y. Mohamed, I.S. Ahmed, N.M. Mohamed, M. Khatab, Hydrothermally synthesized Co3O4, α-Fe2O3, and CoFe2O4 nanostructures: efficient nano-adsorbents for the removal of orange G textile dye from aqueous media, J. Inorg. Organomet. Polym Mater., 27 (2017) 1526-1537.

[3] M.Y. Nassar, A.A. Ali, A.S. Amin, A facile Pechini sol–gel synthesis of TiO2/Zn2TiO2/ZnO/C nanocomposite: an efficient catalyst for the photocatalytic degradation of Orange G textile dye, RSC Adv., 7 (2017) 30411-30421.

[4] M.Y. Nassar, I.S. Ahmed, I. Samir, A novel synthetic route for magnesium aluminate (MgAl2O4) nanoparticles using sol–gel auto combustion method and their photocatalytic properties, Spectrochim. Acta, Part A, 131 (2014) 329-334.

[5] H.V. Vasei, S.M. Masoudpanah, M. Adeli, M.R. Aboutalebi, Solution combustion synthesis of ZnO powders using CTAB as fuel, Ceram. Int., 44 (2018) 7741-7745.

[6] I.S. Ahmed, H.A. Dessouki, A.A. Ali, Synthesis and characterization of new nano-particles as blue ceramic pigment, Spectrochim. Acta, Part A, 71 (2008) 616-620.

[7] I.S. Ahmed, S.A. Shama, M.M. Moustafa, H.A. Dessouki, A.A. Ali, Synthesis and spectral characterization of CoxMg1−xAl2O4 as new nano-coloring agent of ceramic pigment, Spectrochim. Acta, Part A, 74 (2009) 665-672.

[8] X. Wang, M. Qin, F. Fang, B. Jia, H. Wu, X. Qu, A.A. Volinsky, Solution combustion synthesis of nanostructured iron oxides with controllable morphology, composition and electrochemical performance, Ceram. Int., 44 (2018) 4237-4247.

[9] R. Ianoş, C. Păcurariu, S.G. Muntean, E. Muntean, M.A. Nistor, D. Nižňanský, Combustion synthesis of iron oxide/carbon nanocomposites, efficient adsorbents for anionic and cationic dyes removal from wastewaters, J. Alloys Compd., 741 (2018) 1235-1246.

[10] I. Ahmed, H. Dessouki, A. Ali, Synthesis and characterization of new nano-particles as blue ceramic pigment, Spectrochim. Acta, Part A, 71 (2008) 616-620.

[11] I. Ahmed, H. Dessouki, A. Ali, Synthesis and characterization of NixMg1− xAl2O4 nano ceramic pigments via a combustion route, Polyhedron, 30 (2011) 584-591.

[12] A.A. Ali, B. Karasu, M.R. Allazov, T.M. Ilyasli, Synthesis and study of CexPrxMg1-2xAl2O4 ceramic pigment by combustion method using malonic acid dihydrazide as fuel, Int. J. Sci. Eng. Res, 4 (2013) 1686-1690.

[13] A. Ali, B. Karasu, M. Allazov, T. Ilyasli, Synthesis, Characterization and Study of the Effect of Yb 3 on MgAl2O4 Spinel Structure via Combustion Method, J. Chem., DOI (2013) 133.

[14] D. Jinmori, Y. Masubuchi, S. Kikkawa, Magnetic porous iron oxide monoliths prepared through epoxide-mediated sol-gel process, Mater. Res. Bull., 88 (2017) 214-217.

[15] D.-W. Zeng, R. Xiao, J.-M. Zeng, H.-Y. Zhang, Liquid foam assisted sol–gel synthesis of iron oxides for hydrogen storage via chemical looping, Int. J. Hydrogen Energy, 41 (2016) 13923-13933.

[16] J. Xu, S. Thompson, E. O'Keefe, C.C. Perry, Iron oxide–silica nanocomposites via sol–gel processing, Mater. Lett., 58 (2004) 1696-1700.

[17] P. Bhavani, C.H. Rajababu, M.D. Arif, I.V.S. Reddy, N.R. Reddy, Synthesis of high saturation magnetic iron oxide nanomaterials via low temperature hydrothermal method, J. Magn. Magn. Mater., 426 (2017) 459-466.

[18] A. Lassoued, M.S. Lassoued, B. Dkhil, S. Ammar, A. Gadri, Synthesis, photoluminescence and Magnetic properties of iron oxide (α-Fe2O3) nanoparticles through precipitation or hydrothermal methods, Physica E, 101 (2018) 212-219.

[19] Y. Kamei, K. Wakayama, Y. Makinose, Y. Endo, N. Matsushita, Syntheses of iron oxide nanoplates by hydrothermal treatment of iron-oleate precursor and their magnetization reversal, Mater. Sci. Eng., B, 223 (2017) 70-75.

[20] F. Yazdani, M. Seddigh, Magnetite nanoparticles synthesized by co-precipitation method: The effects of

various iron anions on specifications, Mater. Chem. Phys., 184 (2016) 318-323.
[21] W. Tangwatanakul, C. Sirisathitkul, W. Limphirat, R. Yimnirun, Synchrotron X-ray absorption of iron oxide (Fe2O3) nanoparticles: Effects of reagent concentration and sonication in co-precipitation synthesis, Chin. J. Phys, 55 (2017) 845-852.
[22] K. Pušnik, T. Goršak, M. Drofenik, D. Makovec, Synthesis of aqueous suspensions of magnetic nanoparticles with the co-precipitation of iron ions in the presence of aspartic acid, J. Magn. Magn. Mater., 413 (2016) 65-75.
[23] P. Bhavani, C. Rajababu, M. Arif, I.V.S. Reddy, N.R. Reddy, Synthesis of high saturation magnetic iron oxide nanomaterials via low temperature hydrothermal method, J. Magn. Magn. Mater., 426 (2017) 459-466.
[24] M. Tadić, N. Čitaković, M. Panjan, Z. Stojanović, D. Marković, V. Spasojević, Synthesis, morphology, microstructure and magnetic properties of hematite submicron particles, J. Alloys Compd., 509 (2011) 7639-7644.
[25] M. Tadic, N. Citakovic, M. Panjan, B. Stanojevic, D. Markovic, Đ. Jovanovic, V. Spasojevic, Synthesis, morphology and microstructure of pomegranate-like hematite (α-Fe2O3) superstructure with high coercivity, J. Alloys Compd., 543 (2012) 118-124.
[26] M.T.C. Fernandes, R.B.R. Garcia, C.A.P. Leite, E.Y. Kawachi, The competing effect of ammonia in the synthesis of iron oxide/silica nanoparticles in microemulsion/sol–gel system, Colloids Surf., A, 422 (2013) 136-142.
[27] R. Ianoș, E.-A. Moacă, A. Căpraru, R. Lazău, C. Păcurariu, Maghemite, γ-Fe2O3, nanoparticles preparation via carbon-templated solution combustion synthesis, Ceram. Int., DOI https://doi.org/10.1016/j.ceramint.2018.04.258(2018).
[28] M. Huang, M. Qin, Z. Cao, B. Jia, P. Chen, H. Wu, X. Wang, Q. Wan, X. Qu, Magnetic iron nanoparticles prepared by solution combustion synthesis and hydrogen reduction, Chem. Phys. Lett., 657 (2016) 33-38.
[29] M.Y. Nassar, I.S. Ahmed, T.Y. Mohamed, M. Khatab, A controlled, template-free, and hydrothermal synthesis route to sphere-like α-Fe 2 O 3 nanostructures for textile dye removal, RSC Adv., 6 (2016) 20001-20013.
[30] P. Naderi, S. Masoudpanah, S. Alamolhoda, Magnetic properties of Li0. 5Fe2. 5O4 nanoparticles synthesized by solution combustion method, Appl. Phys. A, 123 (2017) 702.
[31] L.A.d. Silva, S.M.S. Borges, P.N. Paulino, M.A. Fraga, S.T.d. Oliva, S.G. Marchetti, M.d.C. Rangel, Methylene blue oxidation over iron oxide supported on activated carbon derived from peanut hulls, Catal. Today, 289 (2017) 237-248.
[32] Y.-S. Li, J.S. Church, A.L. Woodhead, Infrared and Raman spectroscopic studies on iron oxide magnetic nano-particles and their surface modifications, J. Magn. Magn. Mater., 324 (2012) 1543-1550.
[33] N.T. McDevitt, W.L. Baun, Infrared absorption study of metal oxides in the low frequency region (700-240 cm−1), Spectrochim. Acta, 20 (1964) 799-808.